



Cite this: *Soft Matter*, 2019, 15, 7832

Whispering gallery mode lasing in mesomorphic liquid crystal microdroplets

Junaid Ahmad Sofi,  Abinash Barthakur and Surajit Dhara *

In recent years, investigation on the non-display applications of liquid crystals has increased considerably. One of the emerging applications is whispering gallery mode (WGM) lasing. Here, we report experimental studies on the morphology and WGM lasing in nematic (N), smectic-A (SmA) and smectic-C (SmC) microdroplets dispersed in a highly transparent and low refractive index perfluoropolymer. The mesomorphic microdroplets, obtained by varying the temperature, exhibit radial director configuration. The SmA microdroplets are found to be highly stable and robust against mechanical stress compared to the N and SmC microdroplets. We study lasing properties such as intensity, threshold pump energy and linewidth, and show that overall the SmA microdroplets are superior to the N and SmC microdroplets. The experimental results are discussed based on the orientation of the dye molecules, director fluctuations and tilting at the interface.

Received 6th June 2019,
Accepted 5th September 2019

DOI: 10.1039/c9sm01132c

rsc.li/soft-matter-journal

I. Introduction

The quest for the successful realization of flexible and integrated photonic devices has drawn a great deal of interest in recent years. Such devices require tunable optical microcomponents such as filters, sensors and waveguides. In this context, liquid crystal based optical microcomponents are prospective contenders for future generation tunable microdevices.^{1–7} Liquid crystals exhibit a variety of mesophases with distinct optical properties and each mesophase might offer a unique technological solution for specific devices. Microdroplets of a dye-doped liquid crystal act as optical microcavities and recently several studies have been reported.^{5,8–12} In those systems, the light coupled to the microcavity circulates inside due to the total internal reflection and the optical resonance occurs when the circulating light meets in-phase, which is known as whispering gallery mode (WGM) resonance.¹³ Under a simple approximation, this can be achieved when $2\pi n_s a \approx l\lambda$, where a is the radius, n_s is the refractive index of the sphere and l is an integer. If the input energy exceeds a certain threshold, the dye gives off stimulated emission and the microresonator begins to emit multi-mode laser light.

The first report on the WGM resonance by Humar *et al.* opened up a new direction of application of liquid crystals.¹ They demonstrated tunability of WGM resonance, Bragg cavity lasing and surfactant sensing.^{1–3} Peddireddy *et al.* demonstrated lasing and waveguiding in smectic-A liquid crystal fibers.⁴ Petriashvili *et al.* have shown omnidirectional lasing in cholesteric microdroplets.¹⁴ We have reported electrical and

thermal tuning of WGM resonance of nematic microdroplets and the magnetic field tuning of lasing from ferromagnetic nematic microdroplets.^{8,9} Recently, Sofi *et al.* have studied the stability of nematic microdroplets in several dispersing media.¹² There are also many experimental and theoretical reports on liquid crystal microdroplets.^{15–22} Despite rich and diverse structures of liquid crystals, no comparative study has been reported so far with an aim to bring out the relative merits of lasing in the mesomorphic microdroplets. In this paper, we report on the lasing properties of nematic (N), smectic-A (SmA) and smectic-C (SmC) microdroplets of a liquid crystal compound. We show that the SmA microdroplets are mechanically robust and have lower lasing threshold pump energy and higher lasing intensity than that of N and SmC counterparts. Hence, SmA microdroplets are more appealing microcavities for making microlasers. We discuss the possible effects of refractive index contrast, director fluctuations and orientation of the transition dipole moment of the dye molecules on the lasing properties. This study provides useful guidelines for an appropriate choice of liquid crystal mesophase for optical microcavities in diverse photonic applications.

II. Experimental

We used a pyridine derivative liquid crystal compound that exhibits the following phase transitions: I 68 °C N 64.5 °C SmA 57.7 °C SmC 33.2 °C Cr. It exhibits a first order I to N and a second order SmA–SmC phase transition.²³ A small amount of Nile red fluorescent dye (0.7 wt%) was doped in the liquid crystal for inducing fluorescence. The transition dipole moment of the dye molecule is along the long axis.^{24,25} We used a perfluoropolymer

School of Physics, University of Hyderabad, Hyderabad-500046, India.
E-mail: sdsp@uohyd.ernet.in

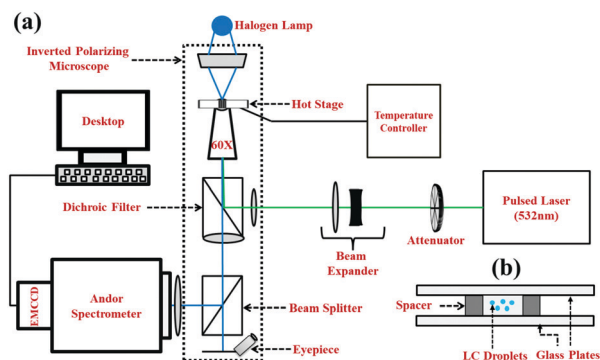


Fig. 1 (a) Schematic diagram of the experimental setup built on an inverted polarising optical microscope. A Q-switched pulsed laser of wavelength 532 nm triggered by the function generator is used to induce the fluorescence emission of the Nile-red dye doped microdroplets. The spectrum emitted from the microdroplets is detected and recorded by the Andor spectrometer, and the images are taken by the camera. (b) Side-view of the cell showing suspended droplets in Cytop solution.

(CTX-809A) commonly known as Cytop as a dispersing medium. It is highly transparent and its refractive index is very low ($n = 1.34$).^{12,26} To reduce the viscosity of the Cytop, we added a fluorinated solvent (CT-Sol.180) with a volumetric ratio of 1 : 2. Cytop is diluted by fluorinated solvent to ease the formation of liquid crystal microdroplets. Both the materials are obtained from Asahi Glass Co. Ltd, Japan. The diluted mixture is named here as “Cytop-solution”. The Cytop-solution containing microdroplets, prepared through micropipette injection, is inserted in a cell prepared by two glass plates which are separated by a spacer of thickness 240 μm (Fig. 1(b)). The liquid crystal is immiscible in Cytop solution. The microdroplets are formed in the nematic phase and cooled slowly to the SmA and SmC phases respectively. The experimental setup is built on an inverted polarising optical microscope (Nikon, Eclipse Ti-U) (Fig. 1(a)). A temperature controller and a heating stage (Instec Inc. mk1000) mounted on the microscope are used to control the temperature with an accuracy of 0.1 $^{\circ}\text{C}$. An isolated microdroplet of desired diameter is selected and pumped with a Q-switched pulsed laser (400 ps) of wavelength 532 nm (Teem Photonics, Model: PNG-M02010-130). The absorption band of Nile red dye matches with the wavelength of the pulsed laser and the fluorescence light is coupled into the microdroplets. All the experiments are performed using a Nikon S Plan Fluor 60 \times /0.70 objective. A high resolution spectrometer (Andor, Shamrock SR-500i) is connected to one of the ports of the microscope and the same objective is used to collect the emission spectrum.^{8,12}

III. Results and discussion

Our experiment starts with the search for an appropriate dispersing medium for liquid crystal microdroplets that provides radial anchoring of the director (the mean orientation direction of the elongated molecules). We tried forming microdroplets in several polymers such as polydimethylsiloxane (PDMS), glycerol-lecithin mixture and the Cytop solution. From the comparative study, it is found that the Cytop-solution provides a perfect radial

anchoring of the director. The radial anchoring is strong and retained over several weeks, without any observable change in the texture. The radial anchoring of the molecules at the interface is due to the very low surface energy of Cytop.^{26,27} There are several studies reported on the alignment behaviour of liquid crystals in Cytop-solution coated Hele-Shaw type cells. It was reported that Cytop-solution provides perfect homeotropic alignment for SmA liquid crystals compared to the conventional homeotropic aligning agents.^{26,28–30} To check the mechanical stability, we applied mild physical stress on the microdroplets with the help of a mechanical tweezer. It is observed that the textures of N and SmC microdroplets are changed irreversibly whereas the SmA microdroplets remain intact after the stress is removed. We did not observe any diffusion of liquid crystal or dye molecules across the interface, except in the isotropic phase. In addition, there is no sedimentation of microdroplets and also no noticeable change in the diameter of the microdroplets is observed across the phase transitions. Thus, SmA microdroplets in Cytop-solution are chemically stable and mechanically robust than N and SmC microdroplets. Fig. 2(a–c) shows the POM micrographs and corresponding λ -plate (530 nm) images of the microdroplets. Four intensity extinction brushes and a hedgehog point defect at the centre indicates that the director is radial (homeotropic) to the interface. This also means that the smectic layers are concentric in both the SmA and SmC microdroplets as shown schematically in Fig. 2(e and f). We noticed that the radial anchoring is partially broken close to the SmC to Cr phase transition (33.2 $^{\circ}\text{C}$) and eventually no lasing is observed. Hence, the experiments on the SmC microdroplets are performed just 5 $^{\circ}\text{C}$ below the SmA–SmC phase transition (which is about 20 $^{\circ}\text{C}$ above the SmC to Cr phase transition temperature).

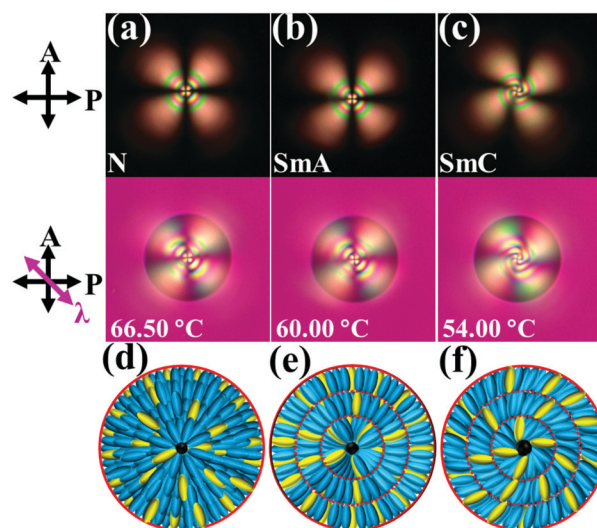


Fig. 2 (a–c) Polarizing optical micrographs (POM) of a microdroplet of diameter 14.5 μm in the N, SmA and SmC phases. λ -Plate images of the respective microdroplets are shown underneath. Temperatures of the microdroplets are shown on the λ -plate images. Crossed polarisers and λ -plate orientation are shown on the left side. (d–f) Schematic director profiles in N, SmA and SmC microdroplets. Yellow ellipsoids represent Nile red dye molecules (doped).

In SmC microdroplets (Fig. 2(c)), the extinction brushes rotate clockwise due to the collective tilting of the molecules in the layers. We have measured the approximate tilt angle (θ) from the POM micrographs at different temperatures below the SmA–SmC phase transition. Fig. 3(a) shows that the tilt angle increases gradually from $\theta = 0^\circ$ to about $\theta = 18^\circ$ as the temperature is decreased from 58°C to 53°C . We also measured the birefringence (Δn) of the sample using a phase modulation technique.^{31–33} Fig. 3(b) shows that Δn increases with decreasing temperature and changes slope discontinuously at the I–N and N–SmA phase transitions. A small but measurable change in Δn is also observed across the SmA–SmC phase transition temperature.

In what follows, we investigate the WGM lasing of the mesomorphic microdroplets. For this purpose about 0.7 wt% Nile red dye was dissolved in the isotropic phase of the liquid crystal before dispersing it in the Cytop-solution to form microdroplets. We choose an isolated microdroplet and illuminate its edge with the tightly focussed laser beam to induce fluorescence. The emitted light is coupled and circulates within the microdroplets due to the total internal reflection, and consequently the WGMs are excited. A representative spectrum of a typical WGM resonance (below the lasing threshold pump energy) of a microdroplet of diameter $10\ \mu\text{m}$ is shown in Fig. 4. When the pumping energy exceeds a certain threshold value, some of the modes start lasing. Fig. 5(a–c) show fluorescence images of microdroplets (diameter $> 20\ \mu\text{m}$) illuminated by pumping energies much above the lasing threshold values. In each microdroplet, we see a brighter light spot on the diametrically opposite side of the excited edge and a thin ring of

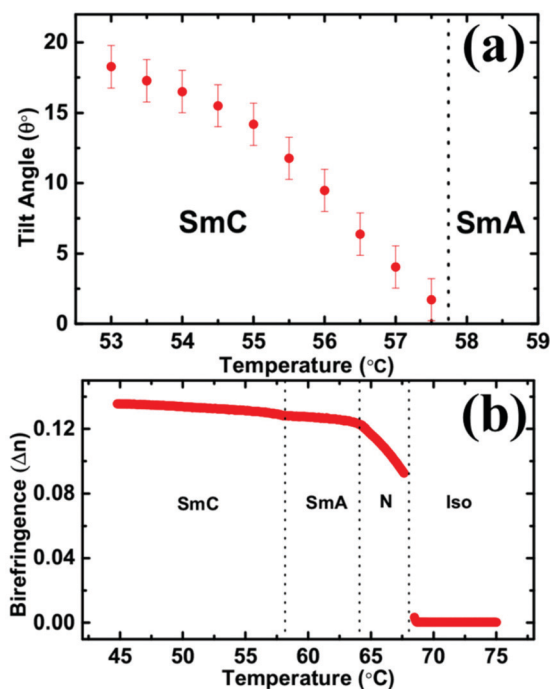


Fig. 3 (a) Temperature dependent tilt angle (θ) measured from the texture of a SmC microdroplet of diameter $33\ \mu\text{m}$. (b) Temperature dependent birefringence (Δn).

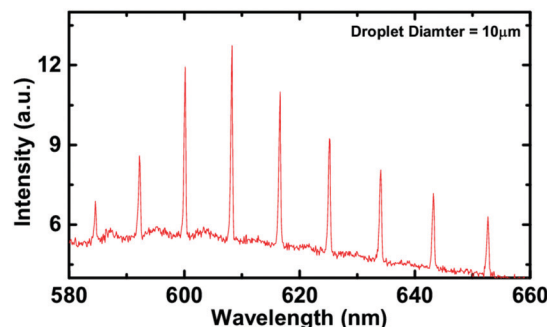


Fig. 4 A typical WGM spectrum at a pumping energy of 20 nJ (below the lasing threshold) of a SmA microdroplet of diameter $10\ \mu\text{m}$.

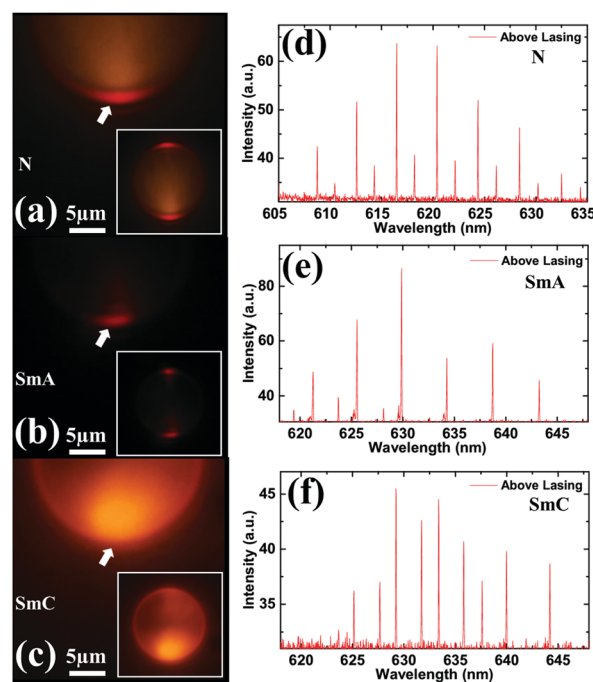


Fig. 5 (a–c) Fluorescence images of illuminated edges of N, SmA and SmC microdroplets with pump energy of 115 nJ. Insets of images (a), (b) and (c) show the respective emission patterns of the whole microdroplets. The N, SmA and SmC microdroplet diameters are 21, 22 and $22.4\ \mu\text{m}$ respectively. (d–f) Emission spectrum from the respective microdroplets. White arrows indicate the excitation edges of the microdroplets.

light within the microdroplet circumference, suggesting the WGM excitation. In addition, a speckle formation is also observed above the lasing threshold pump energy, suggesting that the emitted light is coherent. It is observed that at the illumination point which is just inside the interface, the scattering of light from the SmC microdroplets is comparatively larger than that of N and SmA microdroplets (inset to Fig. 5(c)). The emission spectrum of the respective microdroplets in the lasing regime is also shown in Fig. 5(d–f). It may be noted that the linewidths (FWHM) of the laser lines are much narrower than that of the WGM resonance (Fig. 4). The cavity quality factor of a resonator is given by $Q = \lambda/\Delta\lambda$, where $\Delta\lambda$ is the full-width at half maximum. The quality factor above the lasing threshold pump energy for a fixed droplet size is found to be $Q \sim 10^4$. Two types of peaks with higher and lower intensities are

observed in Fig. 5(d–f). They are considered to be TM and TE modes corresponding to the electric field of the light being either parallel or perpendicular to the director. The long axes of the Nile red molecules and hence the emission transition dipole moments are aligned along the director (yellow ellipsoids in Fig. 2(d–f)). Consequently, the TM modes are strongly coupled to the transition dipole moment and have higher intensities than TE modes in N and SmA microdroplets. However, in SmC the situation is complicated because of the molecular tilt. The transition dipole moments have a projection on to the TE modes and as a result TE modes are enhanced and TM modes are reduced as the temperature is decreased across the SmA to SmC transition.

To investigate the lasing properties, we analysed the most intense modes in three mesomorphic microdroplets. Fig. 6 shows the quantitative differences of the lasing characteristics of N, SmA and SmC microdroplets. In all microdroplets, a typical two-slope curve for intensity and linewidth as a function of pumping energy is observed. The lasing intensity increases and the linewidth decreases with the increasing pump energy. The change of slope occurs at the threshold energy, which suggests the onset of the stimulated emission of the gain medium. During such an emission transition, the gain of the active medium supersedes the optical losses in the microdroplets on account of the attainment of the population inversion between the ground and the excited state energy levels of the dye molecules. In the nematic microdroplet (diameter 21 μm), the lasing threshold pump energy for the highest intensity mode is 75 nJ (Fig. 6(a)). For the SmA and SmC microdroplets (diameter \approx 22 μm) the threshold energies are almost the same *i.e.*, nearly 42 nJ (Fig. 6(c and e)). The variation of the corresponding linewidths is also shown in Fig. 6(b, d and f). A clear change of slope is

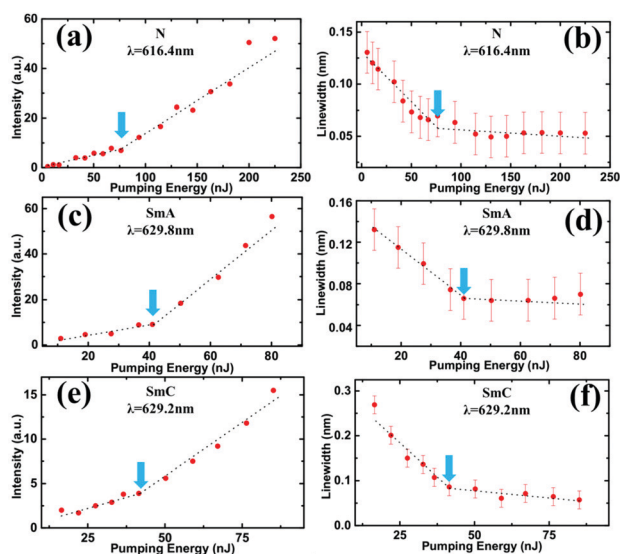


Fig. 6 (a, c and e) Variation of output intensity and (b, d and f) corresponding linewidths as a function of pumping energy. The wavelengths of selected highest intensity modes are 616.4 nm, 629.8 nm and 629.2 nm for the N, SmA and SmC microdroplets respectively. The N, SmA and SmC microdroplets' diameters are 21, 22 and 22.4 μm respectively. Threshold pump energies are marked by arrows. Dotted lines are drawn as guides to the eyes.

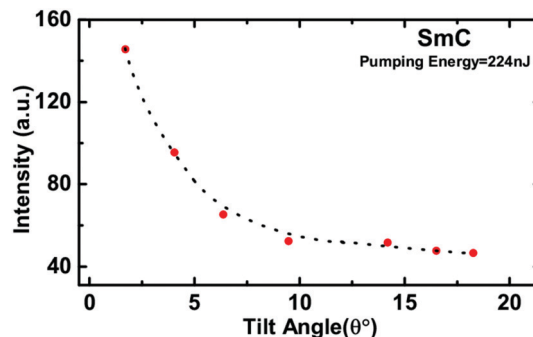


Fig. 7 Variation of lasing intensity of the mode corresponding to the emission line $\lambda = 629.2$ nm with tilt angle θ in the SmC phase for a pumping energy of 224 nJ. A dotted line is drawn as a guide to the eye. Droplet diameter: 25 μm .

observed at the corresponding threshold pump energies. Fig. 6(a, c and e) also show that the lasing intensity from the SmA microdroplet is larger than that from both the N and SmC microdroplets. For example, at a fixed pump energy of 80 nJ (above the threshold pumping energy) the output intensity of the SmA microdroplet is 55 (a.u.) (Fig. 6(c)), whereas in N and SmC microdroplets it is about 10 (a.u.) and 13 (a.u.), respectively (Fig. 6(a and e)). Thus, the intensity of SmA microdroplets is almost 5 times larger than that of the N and SmC microdroplets. In the SmC phase the lasing intensity depends on the tilt angle θ as shown in Fig. 7. The intensity decreases with increasing tilt angle. We also studied the effect of the droplet size on the lasing threshold and the results are shown in Fig. 8(a). The radiation loss due to the curvature in smaller microdroplets is larger than that of the bigger microdroplets as a result of which the threshold energy decreases with increasing diameter. The lasing threshold pumping energy of the N and SmA decreases faster than for the SmC microdroplets. The threshold pump energy of larger SmA microdroplets (diameter > 25 μm) is smaller compared to both the N and SmC microdroplets.

Uniaxial liquid crystals possess extraordinary (n_e) and ordinary (n_o) refractive indices which are temperature dependent and in calamitic liquid crystals, $n_e > n_o$. In mesomorphic compounds,

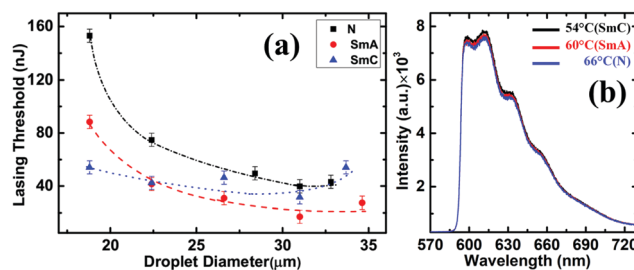


Fig. 8 (a) Dependence of lasing threshold pump energy on microdroplet diameter. Dotted lines are drawn as guides to the eye. (b) Fluorescence intensity measured from a thin film of sample confined between two glass plates at different temperatures. The bandwidth of the excitation filter is 510–560 nm. Small oscillations overlaying the emission are due to the finite thickness of the cell.

usually n_e increases and n_o decreases while decreasing the temperature across the N–SmA–SmC phase transitions. Hence, the refractive index difference ($n_e - n_p$, where n_p is the refractive index of the Cytop-solution) across the SmA–SmC phase transition is increasing. But the SmC phase has monoclinic symmetry and is thus weakly biaxial due to the tilting of the molecules in the layer. With decreasing temperature, θ increases and the intensity of the TM modes (peaks with higher intensities) decreases. The director fluctuations in the nematic microdroplets cause scattering losses in the microcavity. In the SmA microdroplets, the fluctuations are suppressed and hence the scattering losses are reduced. Thus, the lower threshold energy and higher lasing intensity of SmA microdroplets could be attributed to the larger refractive index contrast with respect to the Cytop-solution and the lower scattering losses due to the suppression of the director fluctuations. The quantum yield of the fluorescent dye is usually solvent and temperature dependent and this could also contribute to the lasing properties. To see this effect, we have measured the fluorescence intensity from a thin film of the sample confined between two parallel glass plates at different temperatures. However, no noticeable change in the spectrum is observed (Fig. 8(b)). Hence, quantum efficiency of the dye is not responsible for the difference in the lasing properties of the mesomorphic microdroplets.

IV Conclusions

In summary, we have performed a comparative study of the morphology and lasing properties of N, SmA and SmC microdroplets dispersed in Cytop-solution (perfluoropolymer). We find that the SmA microdroplets are chemically stable and mechanically robust compared to the N and SmC microdroplets. The SmA microdroplets have in general lower lasing threshold pump energy than the N and SmC microdroplets. The lasing intensity of the SmA microdroplets is almost five times larger than that of the N and SmC microdroplets. Thus, SmA microdroplets are superior optical microcavities for lasing. The refractive index contrast with respect to the surrounding medium, director fluctuations, orientation of the transition dipole moment of the dye molecules and director tilt have important contributions to the properties of WGM lasing of the mesomorphic microdroplets. We hope that this study will encourage the investigation of the unexplored lasing properties of several liquid crystal phases.

Funding source

This work was supported by the Science and Engineering Research Board of India (EMR/2015/001566), UPE-II, DST/SJF/PSA-02/2014-15, DST-PURSE.

Conflicts of interest

The authors affiliated with this work declare no conflict of interest.

Acknowledgements

JAS acknowledges UGC-BSR for a fellowship. We all acknowledge Prof. R. Dabrowski for providing the liquid crystal compound.

References

- 1 M. Humar, M. Ravnik, S. Pajk and I. Mušević, *Nat. Photonics*, 2009, **3**, 595–600.
- 2 M. Humar and I. Mušević, *Opt. Express*, 2010, **18**, 26995–27003.
- 3 M. Humar and I. Mušević, *Opt. Express*, 2011, **19**, 19836–19844.
- 4 K. Peddireddy, V. S. R. Jampani, S. Thutupalli, S. Herminghaus, C. Bahr and I. Mušević, *Opt. Express*, 2013, **21**, 30233–30242.
- 5 J. D. Lin, M. H. Hsieh, G. J. Wei, T. S. Mo, S. Y. Huang and C. R. Lee, *Opt. Express*, 2013, **21**, 15765–15776.
- 6 M. Humar, *Liq. Cryst.*, 2016, **43**, 1937–1950.
- 7 J. A. Sofi and S. Dhara, *Appl. Phys. Lett.*, 2019, **114**(1–5), 091106.
- 8 J. A. Sofi, M. A. Mohiddon, N. Dutta and S. Dhara, *Phys. Rev. E*, 2017, **96**(1–5), 022702.
- 9 M. Maruša, J. A. Sofi, I. Kvasic, A. Mertelj, D. Lisjak, V. Niranjana, I. Mušević and S. Dhara, *Opt. Express*, 2017, **25**, 1073–1083.
- 10 T. Arun Kumar, M. A. Mohiddon, N. Dutta, N. K. Viswanathan and S. Dhara, *Appl. Phys. Lett.*, 2015, **106**(1–4), 051101.
- 11 P. V. Shibaev, B. Crooker, M. Manevich and E. Hanelt, *Appl. Phys. Lett.*, 2011, **99**(1–3), 233302.
- 12 J. A. Sofi and S. Dhara, *Liq. Cryst.*, 2019, **46**, 629–639.
- 13 K. Vahala, *Optical Microcavities*, World Scientific, 2004.
- 14 G. Petriashvili, M. P. De Santo, R. J. Hernandez, R. Barberi and G. Cipparrone, *Soft Matter*, 2017, **13**, 6227–6233.
- 15 M. Urbanski, C. G. Reyes, J. H. Noh, A. Sharma, Y. Geng, V. S. R. Jampani and J. P. F. Lagerwall, *J. Phys.: Condens. Matter*, 2017, **29**(1–53), 133003.
- 16 T. Porenta, M. Ravnik and S. Žumer, *Soft Matter*, 2017, **7**, 132–136.
- 17 Y. Geng, D. Sec, P. L. Almeida, O. D. Lavrentovich, S. Žumer and M. H. Godinho, *Soft Matter*, 2013, **9**, 7928–7933.
- 18 A. V. Dubtsov, S. V. Pasechnik, D. V. Shmeliova, A. S. Saidgaziev, E. Gongadze, A. Igljic and S. Kralj, *Soft Matter*, 2018, **14**, 9619–9630.
- 19 O. D. Lavrentovich and Sov. Phys. *JEPT*, 1996, **64**(6), 1237–1244.
- 20 M. N. Krakhalev, A. P. Gardymova, O. O. Prishchepa, V. Y. Rudyak, A. V. Emelyanenko, J. H. Liu and V. Y. Zyryanov, *Sci. Rep.*, 2017, **7**(1–10), 14582.
- 21 J. Kim, M. Khan and S. Y. Park, *ACS Appl. Mater. Interfaces*, 2013, **5**, 13135–13139.
- 22 V. Yu. Rudyak, M. N. Krakhalev, V. S. Sutormin, O. O. Prishchepa, V. Ya. Zyryanov, J.-H. Liu, A. V. Emelyanenko and A. R. Khokhlov, *Phys. Rev. E*, 2017, **96**(1–5), 052701.
- 23 M. Rasi, K. P. Zuhail, A. Roy and S. Dhara, *Phys. Rev. E*, 2018, **97**(1–6), 032702.
- 24 A. Kowski, P. Bojarski and B. Kuklinski, *Chem. Phys. Lett.*, 2008, **463**, 410–412.
- 25 M. C. A. Stuart, J. C. Van de Pas and J. B. F. N. Engberts, *J. Phys. Org. Chem.*, 2005, **18**, 929–934.

- 26 S. M. Jeong, J. K. Kim, Y. Shimbo, F. Araoka, S. Dhara, N. Y. Ha, K. Ishikawa and H. Takezoe, *Adv. Mater.*, 2010, **22**, 34–38.
- 27 S. Naemura, *J. Appl. Phys.*, 1980, **51**, 6149–6159.
- 28 T. Arun Kumar, H. Takezoe and S. Dhara, *Jpn. J. Appl. Phys.*, 2011, **50**(1–3), 040203.
- 29 S. Dhara, J. K. Kim, S. M. Jeong, R. Kogo, F. Araoka, K. Ishikawa and H. Takezoe, *Phys. Rev. E: Stat., Nonlinear, Soft Matter Phys.*, 2009, **79**(1–4), 060701.
- 30 J. K. Kim, F. Araoka, S. M. Jeong, S. Dhara, K. Ishikawa and H. Takezoe, *Appl. Phys. Lett.*, 2009, **95**(1–3), 063505.
- 31 P. Sathyanarayana, M. Mathews, Q. Li, V. S. S. Sastry, B. Kundu, K. V. Le, H. Takezoe and S. Dhara, *Phys. Rev. E: Stat., Nonlinear, Soft Matter Phys.*, 2010, **81**(1–4), 010702.
- 32 P. Sathyanarayana, M. C. Varia, A. K. Prajapati, B. Kundu, V. S. S. Sastry and S. Dhara, *Phys. Rev. E: Stat., Nonlinear, Soft Matter Phys.*, 2010, **82**(1–4), 050701.
- 33 P. Sathyanarayana, V. S. R. Jampani, M. Skarabot, I. Mušević, K. V. Le, H. Takezoe and S. Dhara, *Phys. Rev. E: Stat., Nonlinear, Soft Matter Phys.*, 2012, **85**(1–9), 011702.